www.sciencemag.org/344/6184/598/suppl/DC1

Supplementary Materials for

Hippocampal Neurogenesis Regulates Forgetting During Adulthood and Infancy

Katherine G. Akers, Alonso Martinez-Canabal, Leonardo Restivo, Adelaide P. Yiu, Antonietta De Cristofaro, Hwa-Lin (Liz) Hsiang, Anne L. Wheeler, Axel Guskjolen, Yosuke Niibori, Hirotaka Shoji, Koji Ohira, Blake A. Richards, Tsuyoshi Miyakawa, Sheena A. Josselyn,* Paul W. Frankland*

*Corresponding author. E-mail: paul.frankland@sickkids.ca (P.W.F.), sheena.josselyn@sickkids.ca (S.A.J.)

Published 9 May 2014, *Science* **344**, 598 (2014)
DOI: 10.1126/science.1248903

This PDF file includes:

MATERIALS AND METHODS

Animals

All procedures were approved by the Animal Care and Use Committees at the Hospital for Sick Children or Fujita Health University and conducted in accordance with the policies of the Canadian Council on Animal Care (CCAC) and National Institutes of Health (NIH) Guidelines on the Care and Use of Laboratory Animals

Mice. Mice were bred in the animal facilities at the Hospital for Sick Children or Fujita Health University and maintained on a 12 hr light/dark cycle (lights on at 0700 hrs). Day of birth was designated P0. After weaning (P21), mice were group-housed (2-5 per cage) in transparent plastic cages (31 × 17 × 14 cm) with free access to food and water unless otherwise specified. For most experiments, mice were wild-type (WT) male and female F1 hybrids (C57Bl/6NTac × 129S6/SvEvTac).

For a subset of contextual fear conditioning experiments, three different lines of genetically-modified male and female mice were used. (i) LacZ reporter mice were a cross between a nestin-Cre^{ERT2} line and Rosa-LacZ or Rosa-49YFP lines maintained in a C57Bl/6 background. In these mice, injection of tamoxifen (TAM) leads to expression of the LacZ or YFP transgene only in nestin^{+} cells and their progeny (*47*). (ii) TK^{+} mice were maintained in a 129Svev background. In these mice, a modified HSV-1 thymidine kinase (TK) gene is expressed under the control of a nestin promoter (*48*). Administration of ganciclovir (GAN) causes premature DNA chain termination and apoptosis of only nestin^{+} cells. (iii) iKO-p53 mice were a cross between nestin-Cre^{ERT2} and floxed-p53 lines (*49*) maintained in a C57Bl/6 background. In these mice, injection with TAM leads to the deletion of p53 only in nestin^{+} cells. Genotypes were

determined using PCR analysis of tail DNA samples. For the Barnes maze experiment, WT C57Bl/6 mice were implanted with fluoxetine (FLX) or placebo pellets.

Guinea pigs. Hartley guinea pigs were maintained on a 12 hr light/dark cycle (lights on at 0630 hrs) and group-housed (2 per cage) in transparent plastic cages (47 × 35.5 × 21.5 cm) with free access to food and water.

Degus. Octodon degus were bred in-house. They were maintained on a 12 hr light/dark cycle (lights on at 0630 hrs) and group-housed (5-7 per cage) in transparent plastic cages (47 × 35.5 × 21.5 cm) with free access to food and water.

Treatments

Retrovirus. New neurons were labeled using a replication-deficient retroviral vector (based on the Moloney murine leukemia virus) in which a CAG promoter drives green fluorescent protein (GFP) expression (*11*, *50*). This retroviral vector was prepared by transfecting Plat-gp cells with two plasmids containing an amphotropic envelope (vsvg) and the transgene (pCAG-GFP), followed by collection through ultra-speed centrifugation. Plat-E cells were then infected to generate a stable virus-producing cell line, and concentrated virus solution was obtained by ultra-speed centrifugation (average 3.5 × 109 iu/ml). Mice were treated with atropine (0.1 mg/kg) and anesthetized with chloral hydrate (400 mg/kg). Using stereotaxic procedures, 0.5 µl retrovirus was infused into the dentate gyrus (DG) bilaterally (-2.2 mm AP, ±1.8 mm ML, and 2.2 mm DV relative to bregma) with a glass micropipette. A pump maintained the infusion rate at 0.15 µl/min, and the pipette was left in place for 5 min after each infusion. Mice were postoperatively treated with ketoprofen (5 mg/kg) and perfused 4 weeks later.

Running. Mice in running groups were given voluntary access to a single running wheel placed in their home cages. Mice ran an average of 4.7 km ± 0.53 per day, similar to previous experiments (e.g., (*27*)). In one experiment, the wheel was locked to prevent running. Degus in running groups were given voluntary access to 1-2 custom-made running wheels placed in their home cages. Mice and degus in sedentary groups were similarly housed but not given running wheels.

BrdU. BrdU was dissolved in phosphate-buffered saline (PBS) and injected (100 mg/kg, i.p.) into mice twice per day (12 h apart) for 5 consecutive days.

Ganciclovir. GAN was mixed into powdered food (0.08%) and given to mice *ad libitum*, resulting in an average dose of ~70/mg/kg/day (*30*).

Tamoxifen. TAM was dissolved in sunflower seed oil containing 10% ethanol and injected (180 mg/kg, i.p.) into mice once per day for 5 consecutive days.

Memantine. Memantine (MEM) was dissolved in 0.9% saline and injected (25 mg/kg, i.p.) into mice, guinea pigs, or degus once per week (*31*).

Fluoxetine. FLX (15 mg/kg/day, 21-day release) or placebo pellets were implanted subcutaneously in the dorsal interscapular region of mice under chloral hydrate anesthesia (400 mg/kg) (*51*).

Temozolomide. Temozolomide (TMZ) was dissolved in 0.9% saline containing 10% DMSO. Four rounds of treatment at 1 week intervals were given to mice, with each round consisting of one injection (25 mg/kg, i.p.) per day for 4 consecutive days (*30*).

P7C3. P7C3 was dissolved in deionized water containing 2% DMSO, 8% Cremaphor, and 5% dextrose (pH 7.4) and injected once per day (25 mg/kg, i.p.) for 28 days (*52*).

Behavioral Testing

Contextual Fear Conditioning. For mice, contextual fear conditioning occurred in test chambers (31 cm × 24 cm × 21 cm) with shock-grid floors (bars 3.2 mm in diameter spaced 7.9 mm apart). The front, top and back of the chamber were clear acrylic and the sides were modular aluminum. During training, mice were placed in the chambers, and three foot shocks (0.5 mA, 2 s duration, 1 min apart) were delivered after 2 min. For mice in the strong contextual fear conditioning experiment, five foot shocks (0.5 mA, 2 s duration, 1 min apart) were delivered after 2 min. Mice were removed from the chambers 1 min after the last shock. During the test, mice were placed in the chambers for 5 min. For degus, contextual fear conditioning occurred in test chambers (30.5 × 25.5 × 33 cm) with shock-grid floors (bars 5.0 mm diameter spaced 20.0 mm apart). The front, top and back of the chamber were clear acrylic and the sides were modular aluminum. Degus underwent identical training and testing procedures as mice except that foot shocks were delivered at a higher intensity (2 mA). Behavior was recorded by overhead cameras. Freezing (i.e. absence of movement except for breathing) was measured using automated scoring systems for mice and degus.

Incidental Context Learning Paradigm. Incidental context learning in mice occurred in the same chambers as described above (Med Associates). During the context pre-exposure session, mice were placed in the chambers for 10 min. During the immediate shock session, mice were returned to the chambers, a single foot shock was immediately delivered (≤ 1 s after entry, 1 mA, 2 s duration), and mice were removed from the chambers after 1 min. During the test session, mice were placed in the chambers for 3 min.

Water Maze. For mice, a circular plastic pool (120 cm diameter, 50 cm height) was filled to a depth of 40 cm with water (~26º C) made opaque by the addition of nontoxic paint. A

circular escape platform (10 cm diameter) was submerged 0.5 cm below the surface of the water in the center of one of the pool quadrants. The pool was surrounded by curtains that were located at least 1 m from the pool wall and painted with distinct geometric cues. For guinea pigs, a circular plastic pool (185 cm diameter, 60 cm height) was filled to a depth of 45 cm with water (room temperature) made opaque by the addition of nontoxic paint. A circular escape platform (14 cm diameter) was submerged 2 cm below of the surface of the water. Geometric cues were located on the walls of the room. During training, mice were given 3 trials per day for 4 days, and guinea pigs were given 8 trials per day for 5 days. Trials started when animals were released into the pool, facing the wall, from one of 4 possible points. A different release point was used for each trial on each day, and the order of release points varied pseudorandomly across days. Trials ended when animals reached the hidden platform or 60 s elapsed. If an animal failed to find the platform, it was guided by the experimenter. During the probe tests, the platform was removed from the pool, and animals were allowed to swim for 60 s. Swim paths were recorded by an overhead video camera and tracked using automated software. For mice, latency to reach the platform was recorded during training, and time spent in a circular zone (15 cm radius) centered on the platform location was measured during probe tests. Density plots depicting areas of the pool visited more frequently during the probe tests were generated using a custom program developed in our laboratory. For guinea pigs, latency to reach the platform was recorded during training and probe tests.

Barnes Maze. A white circular platform (100 cm diameter, 70 cm above the floor) contained 12 holes equally spaced around its perimeter. Under one of the holes, there was a black Plexiglas escape box (17 × 13 × 7 cm) filled with paper bedding. The location of this escape hole was consistent for a given mouse but randomized across mice. To prevent navigation based on

olfactory or proximal cues within the maze, the platform was rotated before each trial, and the spatial location of the escape hole remained in a fixed location with respect to the distal room cues. During habituation, mice were allowed 5 min to freely explore the maze, with no escape box present. During training, mice were given 3 trials per day for 6 days. On each trial, mice were released in the center of the maze and allowed 5 min to enter the escape box, where it remained for 30 s. If a mouse failed to find the escape box, it was guided by the experimenter. During probe tests, the escape box was removed from the maze, and mice were allowed to search for 3 min. Time spent around each hole was recorded. Search paths were recorded by an overhead video camera and tracked using automated software based on the public domain NIH ImageJ program and custom modifications of ImageJ software

Conditioned Taste Aversion. During habituation, water-restricted mice were placed in individual cages and given access to two bottles containing tap water for gradually decreasing amounts of time across days: 4 hours on day 1, 2 hours on day 2, 1 hour on day 3, and 30 min on days 4 and 5. During conditioning, the water bottles were replaced by a single bottle containing a saccharin solution (0.1% saccharin in tap water). Mice were allowed to drink for 30 min and then injected with LiCl (0.30M in PBS, 2% body weight, i.p.). During testing, mice were given access to one bottle containing tap water and one bottle containing saccharin solution. During the delay between conditioning and testing, mice were kept on water restriction for 4 days each week, during which they were placed in individual cages and given access to two water bottles for 1 hour a day. Throughout the experiment, a limited amount of wet food was provided daily in the home cage to maintain ~90% of baseline body weight.

Histology

Tissue Preparation. Mice, guinea pigs, and degus were perfused transcardially with PBS followed by 4% paraformaldehyde (PFA). Brains were post-fixed in PFA and transferred to 30% sucrose. Coronal sections (50 μm) were cut along the entire anterior-posterior extent of the DG using a cryostat. Sections were kept in sequential order and stored free-floating in 50% glycerol and 10% ethylene glycol in PBS. A 1/4 section sampling fraction was used to create four sets (each containing sections at 200 μm intervals) for immunohistochemistry.

Immunohistochemistry. Unless otherwise stated, all incubations occurred at room temperature.

For Ki67 labeling, sections were pre-treated with 0.01M citrate buffer (pH 6.0) in a 97º C steamer for 20 min, allowed to cool to room temperature for 20 min, and then treated with 3% H_20_2 in PBS for 10 min. Sections were then incubated with primary (rabbit anti-Ki67, 1:1000) and secondary (biotinylated goat anti-rabbit, 1:1000) antibodies. $Ki67^+$ cells were visualized using avidin-biotin-peroxidase complex (ABC) followed by diaminobenzidine (DAB).

For DCX labeling, sections were pre-treated with 0.01M citrate buffer (pH 6.0) in a 97º C steamer for 20 min and then allowed to cool to room temperature for 20 min. Sections were then incubated with primary (rabbit anti-DCX, 1:1000) and secondary (biotinylated goat anti-rabbit, 1:2000) antibodies. DCX^+ cells were visualized using ABC followed by signal amplification using a TSA system and SAV Alexa-488. DAPI (1:10000) was used as a counterstain.

For GFP labeling and GFP/ZnT3 double-labeling, sections were incubated with primary (rabbit anti-GFP, 1:1000; goat anti-ZnT3, 1:1000) and secondary (donkey anti-rabbit Alexa-488, 1:1000; donkey anti-goat Alexa-568, 1:1000) antibodies. DAPI was used as a counterstain.

For BrdU labeling, sections were pre-treated with 1N HCl at 45°C for 30 min. Sections were then incubated with primary (rat anti-BrdU monoclonal, 1:1000) and secondary (Alexa-488 goat anti-rat, 1:1000) antibodies.

For TUNEL labeling, sections were pre-treated with 0.01M citrate buffer (pH 6.0) in a 97º C steamer for 20 min and allowed to cool to room temperature for 20 min. Sections were then processed using the DeadEnd Colorimetric TUNEL System. Methyl green was used as a counterstain.

For LacZ labeling, sections were incubated with primary (rabbit anti-Laz, 1:1000) and secondary (donkey anti-rabbit Alexa-488, 1:1000) antibodies.

Imaging and Quantification. $Ki67^+$, DCX^+ and $LacZ^+$ cell quantification was performed using an Olympus BX61 microscope and StereoInvestigator 9.0 software. The total number of labeled cells in the DG was estimated using the optical fractionator technique. With a 60× oil-immersion objective (N.A. 1.43), labeled cells were counted inside 90 × 90 μm counting frames equally spaced across a 250 × 250 μm grid with a 20 μm optical dissector height. The counting parameters were chosen to achieve a Gundersen coefficient of error less than 0.1 (*53*). GFP^+ cells in WT mice and DCX^+ cells in FLX-treated mice were counted manually. Data are reported as number of cells per 1000 μm^2.

For quantification of YFP^+ large mossy terminals (LMTs), DCX^+ LMTs, and $ZnT3^+$ puncta, a LSM-710 confocal microscope with a 20× objective (N.A. 0.8) was used to acquire serial Z-stack images (step: 0.8 μm) of the CA3 region at a resolution of 1024 × 1024 pixels (212 × 212 μm, digital zoom: 1×). Using ImageJ software, labeled structures were counted in a 70 × 70 μm square within the stratum lucidum of the CA3b region. Data are reported as number of LMTs per 1000 μm^2.

Three-dimensional reconstructions of GFP^+ LMTs were created using an LSM-710 confocal microscope with Zen 2009 software. With a 63× oil-immersion objective (N.A. 1.40), serial Z-stack images were acquired (step: 0.25 μm). The contours of the GFP^+ LMT and $ZnT3^+$ zone were traced in 3 dimensions using Neurolucida 9.1 software, and surface reconstruction was performed using the 3D visualization module.

$BrdU^+$ and $TUNEL^+$ cell quantification was performed manually using a Nikon microscope. With a 40× objective, $BrdU^+$ cells were counted in the granule cell layer, and $TUNEL^+$ cells were counted from the entire DG. Data are reported as number of cells per section.

Specific experimental procedures

Age differences in hippocampal neurogenesis in mice. To track age-dependent changes in neurogenesis, GFP-expressing retrovirus was infused into the DG of mice at P17 or P60. Mice were perfused 28 days later, and sections were stained for GFP. In a second experiment, mice were perfused at P17, P28, P60, P120, or P180, and sections were stained for Ki67 and DCX.

Age differences in synaptic remodeling in mice. We developed a computational model to estimate differences between P17 and P60 mice in the amount of DG-CA3 synaptic remodeling occurring across time. First, the number of $Ki67^+$ cells in the DG was estimated by fitting a double exponential curve ($Y = (a \times \exp(-b \times X)) + (c \times \exp(-d \times X))$, $r^2 = 0.91$) to the data shown in Fig. 1C. Thirty percent of $Ki67^+$ cells were assumed to survive and mature into granule cells that project mossy fibers to the CA3 and grow LMTs onto CA3 pyramidal cells within 14 days (*54, 55*). Next, the number of LMTs making contact with CA3 cells was calculated by multiplying the number of LMTs per DG cell (n = ~14 (*56, 57*), generated by a Gaussian

function) by the number of DG cells added each day. Finally, the number of new LMTs making contacts with CA3 cells was divided by the total number of LMTs per CA3 cell (n = 50 (*56, 57*)). A CA3 cell was defined as being remodeled if 2-4% of its synaptic inputs were altered by new neuron addition, and cumulative predicted synaptic remodeling was expressed as the proportion of CA3 cells (from a total of 250,000 *(58)*) with altered synaptic inputs as a consequence of new neuron addition.

Age differences in memory persistence in mice. To assess age-dependent changes in memory persistence, separate groups of P17 or P60 mice were trained in contextual fear conditioning and tested 1, 7, 14, or 28 days later. Other groups of control P17 or P60 mice were treated similarly but did not receive foot shocks. These no-shock control mice were similarly tested 1 or 28 days later. Shock reactivity was assessed in a subset of shocked P17 and P60 mice by measuring the distance mice traveled immediately before and during the foot shocks. As a second way to assess age-dependent changes in memory persistence, separate groups of P17 or P60 mice were trained in the incidental context learning paradigm, and immediate shock and test sessions occurred 1, 7, 14, or 28 days later. Age-matched groups of control mice were not exposed to the context prior to immediate shock and test sessions.

Effect of TAM on acquisition of context fear memory. Because we used TAM-inducible transgenic lines (i.e., nestin-Cre^{ERT2} × Rosa-LacZ, nestin-Cre^{ERT2} × floxed-p53) in some experiments, we evaluated whether TAM treatment has acute effects on behavior and neurogenesis. C57Bl/6 mice (the same genetic background as TAM-inducible lines) were treated with TAM or vehicle starting at P60 and then trained in contextual fear conditioning and tested 24 hours later. Mice were then perfused, and sections were stained for DCX.

Effect of running on adult hippocampal neurogenesis in adult mice. To assess whether voluntary running increases neurogenesis, separate groups of mice remained sedentary or were allowed access to a running wheel for 0, 3, 7, 14, or 28 days starting at P60. Mice were then perfused, and sections were stained for Ki67 and DCX. To control for the presence of a novel object in the home cage, a control experiment compared mice that were given a locked running wheel, mice that were allowed to run on an unlocked wheel, and mice that were not given a running wheel (i.e., sedentary) for 28 days. In a second experiment, mice were injected with BrdU starting on P30. Starting on P60, mice remained sedentary or ran for 7 days. Mice were then perfused, and sections were stained for BrdU and TUNEL. In a third experiment, GFP-expressing retrovirus was infused in the DG of mice on P60. Mice then ran for 28 days before being perfused, and sections were stained for GFP and ZnT3 and used for 3-dimensional reconstruction of pre-synaptic terminals in CA3. In a fourth experiment, LacZ/YFP reporter mice (nestin-cre^{ERT2} × YFP reporter mice) were injected with TAM starting at P55, and then remained sedentary or ran for 28 days starting at P60. Mice were then perfused, and sections were stained for GFP and ZnT3.

Effect of running on context fear memory and blockade of the running effect by genetic suppression of neurogenesis in adult mice. To test whether the running-induced increase in neurogenesis leads to forgetting, LacZ reporter mice were injected with TAM starting on P55. Half of the mice underwent contextual fear conditioning on P60, remained sedentary or ran for 42 days, and then were tested. The other half remained sedentary or ran for 42 days before conditioning and testing. Mice were perfused after testing, and sections were stained for LacZ. To test whether running induces forgetting of a stronger context fear memory, mice were trained with five (rather than three) foot shocks on P60, remained sedentary or ran for 28 days, and then

were tested. To test whether preventing the running-induced increase in neurogenesis blocks forgetting, TK^+ mice and their WT littermates were trained in contextual fear conditioning on P60, remained sedentary or ran for 42 days, and then were tested. Both TK^+ and WT mice were placed on GAN-containing food starting 7 days before training and continuing until testing. Mice were perfused after testing, and sections were stained for DCX.

Effect of pharmacological increases in neurogenesis on context fear memory and blockade by genetic suppression in adult mice. Mice underwent contextual fear conditioning on P60. Separate groups were then either given (1) a single injection of MEM or vehicle 24 hours after conditioning with a test session 48 hours after conditioning, (2) weekly injections of MEM or vehicle for 6 weeks with a test session 1 week after the final injection, or (3) weekly injections of MEM or vehicle for 6 weeks with a test session 2 weeks after the final injection. Additional groups of mice were trained in the incidental context learning paradigm on P60, received weekly injections of MEM or vehicle for 4 weeks, and then given shock and test sessions. To test whether preventing the MEM-induced increase in neurogenesis blocks forgetting, TK^+ mice and their WT littermates were trained in contextual fear conditioning on P60, received weekly injections of MEM or vehicle for 42 days, and then were tested. Mice were perfused after testing, and sections were stained for DCX. In a second experiment, mice were subcutaneously implanted with FLX or placebo pellets on P70 and then trained to locate an escape box in the Barnes maze. Probe tests occurred 2 and 30 days after training. Mice were perfused after testing, and sections were stained for DCX.

Effect of genetic increase in neurogenesis on context fear memory in adult mice. iKO-p53 mice and their WT littermates underwent contextual fear conditioning on P60, were treated with

TAM starting the next day, and were tested 28 days later. Mice were perfused after testing, and sections were stained for DCX and Ki67.

Effect of running on other hippocampus-dependent memories in adult mice. To test whether running induces forgetting of a context-only memory, mice were trained in the incidental context learning paradigm on P60, then remained sedentary or ran for 28 days, and then given immediate shock and test sessions. Separate groups of mice remained sedentary or ran for 28 days before training, shock, and test sessions. Mice were perfused after testing, and sections were stained for Ki67. To test whether running induces forgetting of a spatial memory, mice were trained to locate a hidden platform in the water maze starting on P60. An initial probe test occurred immediately after training. Mice then remained sedentary or ran for 28 days, followed by a second probe test.

Effect of running on a hippocampus-independent memory in adult mice. Mice were trained in taste aversion conditioning on P60 and then remained sedentary or ran for 28 days. A test session occurred 28 days after conditioning.

Effect of genetic reduction in neurogenesis on memory in infant mice. TK^+ mice and their WT littermates were administered GAN in their food (which was also available to the dam) starting on P10. On P17, TK^+ and WT mice were trained in contextual fear conditioning and then were tested 1 day or 7 days later. Separate groups of mice were similarly treated (placed in the chamber on P17) but did not receive foot shocks. Mice were perfused after testing, and sections were stained for Ki67 and DCX.

Effect of pharmacological reduction in neurogenesis on memory in infant mice. To test whether reducing neurogenesis mitigates infantile forgetting, P17 mice were trained in the incidental context learning paradigm, then given 4 rounds of injection with vehicle or TMZ, and

then given immediate shock and test sessions. Separate groups of P17 mice were given 4 rounds of injection with vehicle or TMZ before training, shock, and test sessions. Mice were perfused after testing, and sections were stained for Ki67 and DCX. To determine whether reducing cell death alleviates infantile forgetting, mice were trained in the incidental context learning paradigm on P17, then given injections of vehicle or P7C3 for 28 days, and then given immediate shock and test sessions.

Lack of age differences in hippocampal neurogenesis and memory persistence in precocial guinea pigs and degus. To assess hippocampal neurogenesis, degus and guinea pigs were perfused at P17 or P60, and sections were stained for Ki67 and DCX. Levels of neurogenesis were compared to those observed in mice at P17 and P60. To assess memory persistence, degus underwent contextual fear conditioning on P17 or P60 and were tested 1 and 28 days later. Guinea pigs were trained to locate a hidden platform in the water maze starting on P17 or P60 and were tested 1 day or 28 days later.

Effect of running and pharmacological increases in neurogenesis on memory persistence in infant degus and guinea pigs. Degus were trained in contextual fear conditioning on P17 and then either remained sedentary, ran, or received weekly vehicle or MEM injections for 28 days. After testing, degus were perfused, and sections were stained for DCX. Guinea pigs were trained to locate a hidden platform in the water maze, received weekly injections of vehicle or MEM over 4 weeks, and then were tested. Guinea pigs were perfused after testing, and sections were stained for DCX.

Statistical Analysis

Data were analyzed using analysis of variance (ANOVA) and two-tailed *t*-tests. Statistical significance was set at $P < 0.05$. To examine individual-level relationships between measures of neurogenesis and memory, Pearson's *r* was reported after using nonlinear regression to calculate exponential rate of decay ($y = A \times e^{(-k \times x)}$).

SUPPLEMENTAL FIGURES

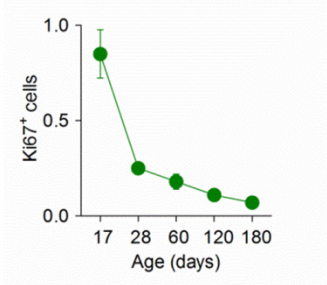

Fig. S1. Age-dependent decrease in proliferation in the DG**.** The number of proliferating ($Ki67^+$) cells in the mouse DG decreased with age (P17 $n = 5$, P28 $n = 5$, P60 $n = 4$, P120 $n = 4$, P180 $n = 4$; *age* main effect, $F_{4,17} = 23.62$, $P < 0.001$).

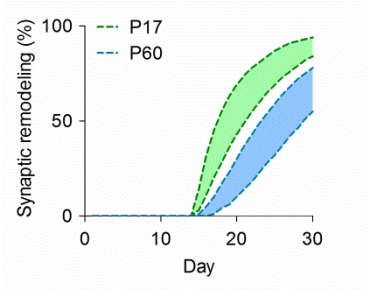

Fig. S2. Computational model of how the addition of new neurons might impact DG-CA3 circuits. During infancy, the addition of many new neurons altered contacts on virtually all CA3 pyramidal cells after one month. By contrast, during adulthood, the addition of fewer new neurons led to more modest synaptic rearrangements.

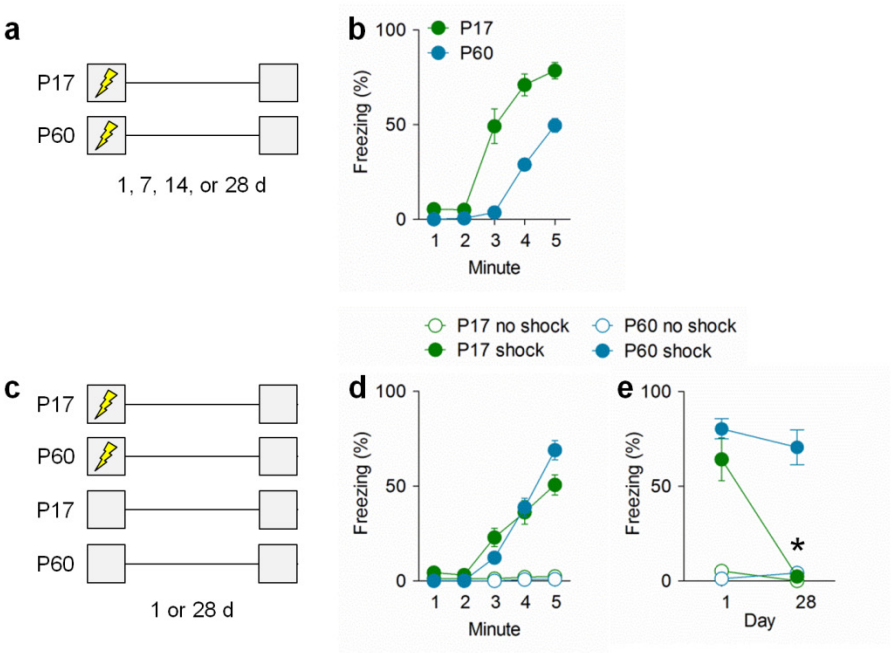

Fig. S3. Forgetting of context fear memory in infant mice. (**a**) Infant (P17) and adult (P60) mice were trained in contextual fear conditioning and then tested 1, 7, 14, or 28 days later. (**b**) During training, infant (n = 36) and adult (n = 34) mice displayed increasing levels of freezing after each foot shock (3 shocks delivered before minutes 3, 4, and 5). (**c**) Infant and adult mice were trained in contextual fear conditioning or placed in the conditioning chamber with no foot shock and then tested 1 or 28 days later. (**d**) During training, shocked mice (P17 n = 12, P60: n = 17) displayed increasing levels of freezing after each foot shock, whereas non-shocked (P17 n = 10, P60: n = 16) mice did not exhibit freezing. (**e**) During testing, shocked adult mice showed stable context fear memory for 28 days (1 day n = 8, 28 days n = 9; 1 vs. 28 days, $P > 0.05$), whereas shocked infant mice showed forgetting (1 day n = 5, 28 days n = 7; 1 vs. 28 days, $t_{10} = 6.52$, $P < 0.001$). Non-shocked infant (1 day n = 4, 28 days n = 6) and adult (1 day n = 8, 28 days n = 8) mice did not exhibit freezing during testing.

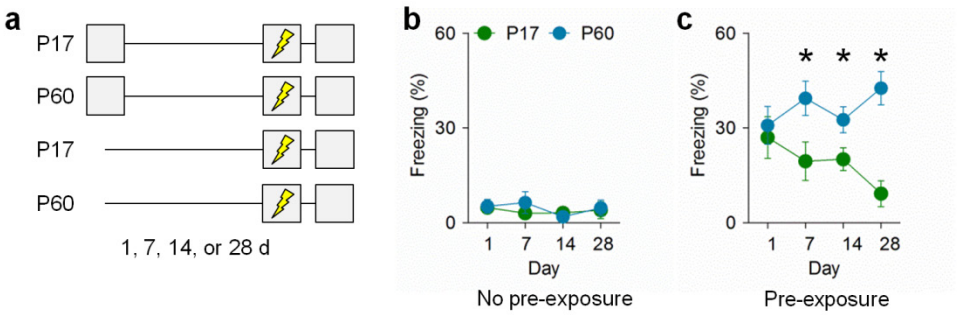

Fig. S4. Forgetting of context-only memory in infant mice. (**a**) Infant (P17) and adult (P60) mice were pre-exposed or not pre-exposed to a context. One, 7, 14, or 28 days later, separate groups of mice received an immediate shock in that context and then were tested the following day. (**b**) Infant and adult mice that were not pre-exposed to the context displayed an immediate shock deficit during testing (n = 8-10 per group). (**c**) Context pre-exposure rescued the immediate shock deficit in adult mice regardless of the delay between context pre-exposure and immediate shock training (n = 13-15 per group). By contrast, context pre-exposure was ineffective in rescuing the immediate shock deficit in infant mice after longer delays (n = 13-15 per group), indicating forgetting of the context-only memory (*age* × *delay* interaction, $F_{3,103} = 2.94$, $P < 0.05$; post hoc t-test, 7 d, $P < 0.05$; 14 d, $P < 0.05$; 28 d, $P < 0.001$).

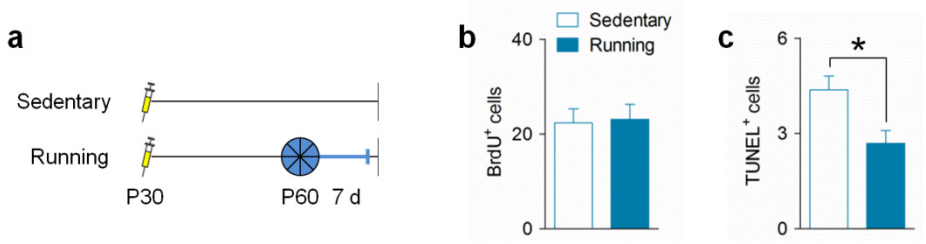

Fig. S5. Running during adulthood does not induce death of developmentally-generated granule cells. (**a**) Adult (P60) mice remained sedentary ($n = 8$) or ran ($n = 8$) after BrdU injection on P30. (**b**) Compared to sedentary mice, running mice showed equivalent numbers of surviving $BrdU^+$ cells and fewer numbers of cells undergoing apoptosis (i.e., $TUNEL^+$; **c**, $t_{14} = 2.82$, $P < 0.05$). These results indicate that running-induced increases in neurogenesis are not associated with increased death of dentate granule cells generated earlier during development.

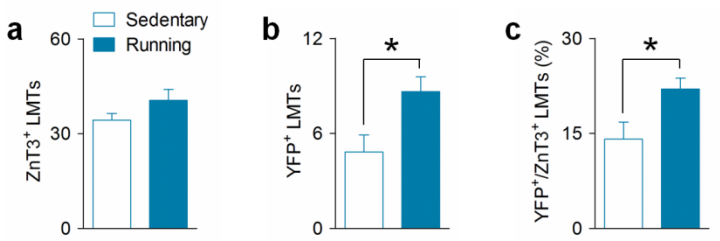

Fig. S6. Running increases the ratio of new-to-established LMTs in the CA3. GFP-expressing retrovirus was injected into the DG of adult (P60) mice to label newborn dentate granule cells and their processes. Mice ran ($n = 6$) or remained sedentary ($n = 6$) for 4 weeks, and tissue was counterstained for ZnT3, a marker of mature presynaptic terminals. (**a**) Numbers of LMTs in the CA3 were equivalent in running and sedentary mice. However, running was associated with an increase in (**b**) number ($t_{10} = 2.67$, $P < 0.05$) and (**c**) proportion ($t_{10} = 2.47$, $P < 0.05$) of newly-generated ($GFP^+/ZnT3^+$) LMTs.

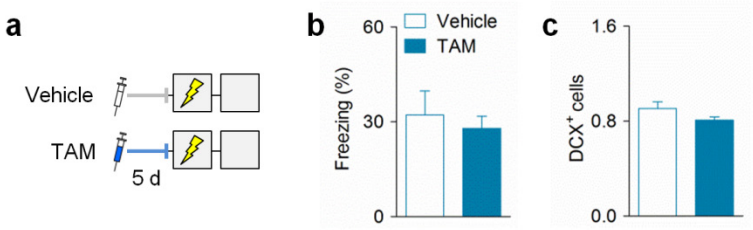

Fig. S7. TAM treatment does not impact context fear memory formation or neurogenesis. (**a**) Adult mice were treated with TAM (n = 8) or vehicle (n = 9) and then trained in contextual fear conditioning. TAM- and vehicle-treated mice showed no differences in (**b**) acquisition of a context fear memory ($P > 0.05$) or (**c**) number of immature (DCX+) neurons in the DG ($P > 0.05$).

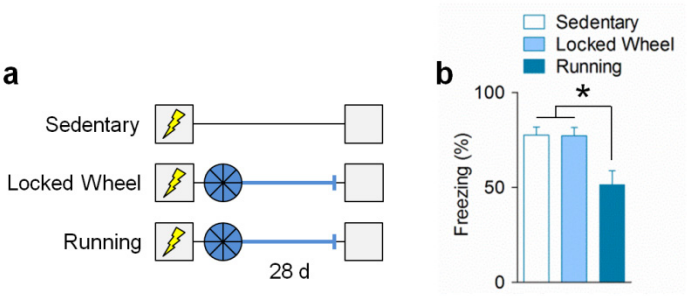

Fig. S8. The presence of a locked running wheel does not lead to forgetting of a context fear memory. (**a**) Adult (P60) mice were trained in contextual fear conditioning then remained sedentary (n = 12), given a locked wheel (i.e., no running; n = 8), or allowed to run (n = 12) for 28 days, after which they were tested. (**b**) Running mice showed less freezing in the trained context compared with sedentary ($t_{22} = 3.08$, $P < 0.01$) or locked wheel ($t_{18} = 2.65$, $P < 0.05$) mice (*group* main effect, $F_{2,29} = 6.95$, $P < 0.01$).

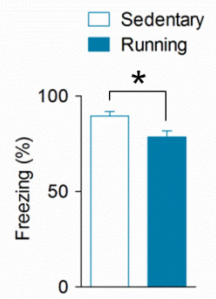

Fig. S9. Running-induced forgetting of a strong context fear memory. Adult (P60) mice were trained with five (rather than three) foot shocks and then ran (n = 10) or remained sedentary (n = 10) for 28 days. Post-learning running induced less (although still significant) forgetting of a strong context fear memory ($t_{18} = 2.71$, $P < 0.05$).

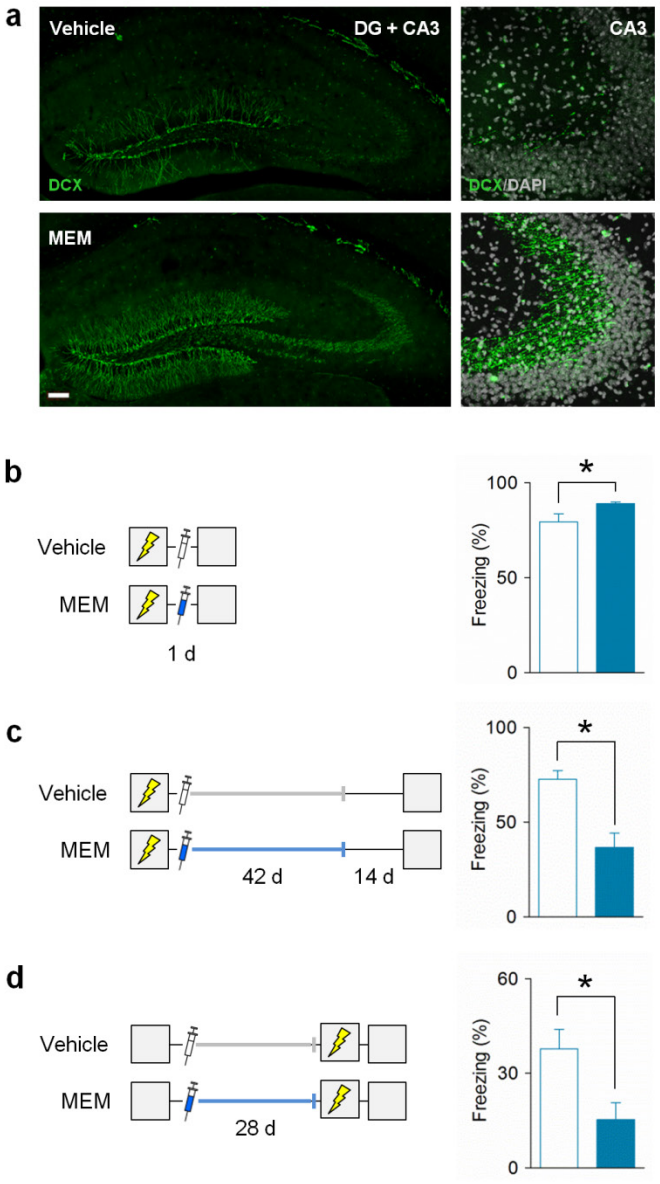

Fig. S10. MEM increases neurogenesis and induces forgetting of context memories in adult (P60) mice. (**a**) MEM treatment (6 injections, spaced 1 week apart) increased the number of DCX^+ cells in the DG (left, scale bar = 100 µm) and DCX^+ processes in the CA3 (right, scale bar = 50 µm) of adult mice. (**b**) A single post-training MEM injection did not disrupt initial consolidation of a context fear memory (MEM $n = 8$, vehicle $n = 8$; $t_{14} = 2.26$, $P < 0.05$). (**c**) Prolonged post-training MEM treatment (6 injections, spaced 1 week apart) resulted in forgetting

of a context fear memory 8 weeks later (MEM $n = 7$, vehicle $n = 7$; $t_{12} = 4.11$, $P = 0.001$) later. (**d**) Prolonged post-training MEM treatment (4 injections, spaced 1 week apart) also resulted in forgetting of a content-only memory (MEM $n = 10$, vehicle $n = 10$; $t_{18} = 2.73$, $P < 0.05$).

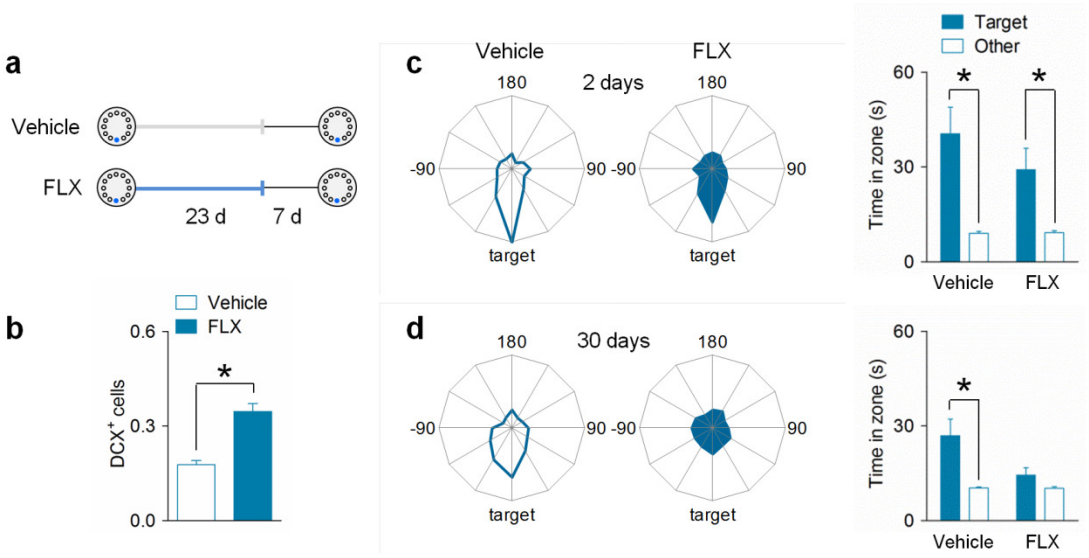

Fig. S11. Fluoxetine (FLX) increases neurogenesis and induces forgetting of a spatial memory in adult (P70) mice. (**a**) Chronic FLX treatment increased the number of DCX^+ cells in the DG (vehicle $n = 5$, FLX $n = 5$; $t_8 = 5.97$, $P < 0.001$). (**b**) Adult mice were treated with vehicle or FLX after learning an escape location in the Barnes maze. (**c**) One day after training, vehicle-treated ($n = 10$) and FLX-treated ($n = 8$) mice showed a spatial bias for the escape location (target) compared to other locations (vehicle, $t_9 = 3.53$, $P < 0.01$; FLX, $t_7 = 2.71$, $P < 0.05$). (**d**) Twenty-eight days after training, vehicle-treated but not FLX-treated mice showed a spatial bias for the escape location (target) compared to other locations (vehicle, $t_9 = 2.96$, $P < 0.05$; FLX, $P > 0.05$).

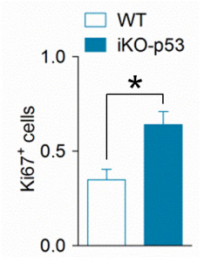

Fig. S12. Inducible deletion of p53 from neural progenitor cells increases proliferation in the DG. Adult (P60) iKO-p53 mice had more proliferating ($Ki67^+$) cells in the DG than WT mice (iKO-p53: $n = 3$, WT: $n = 4$; $t_5 = 3.29$, $P < 0.05$).

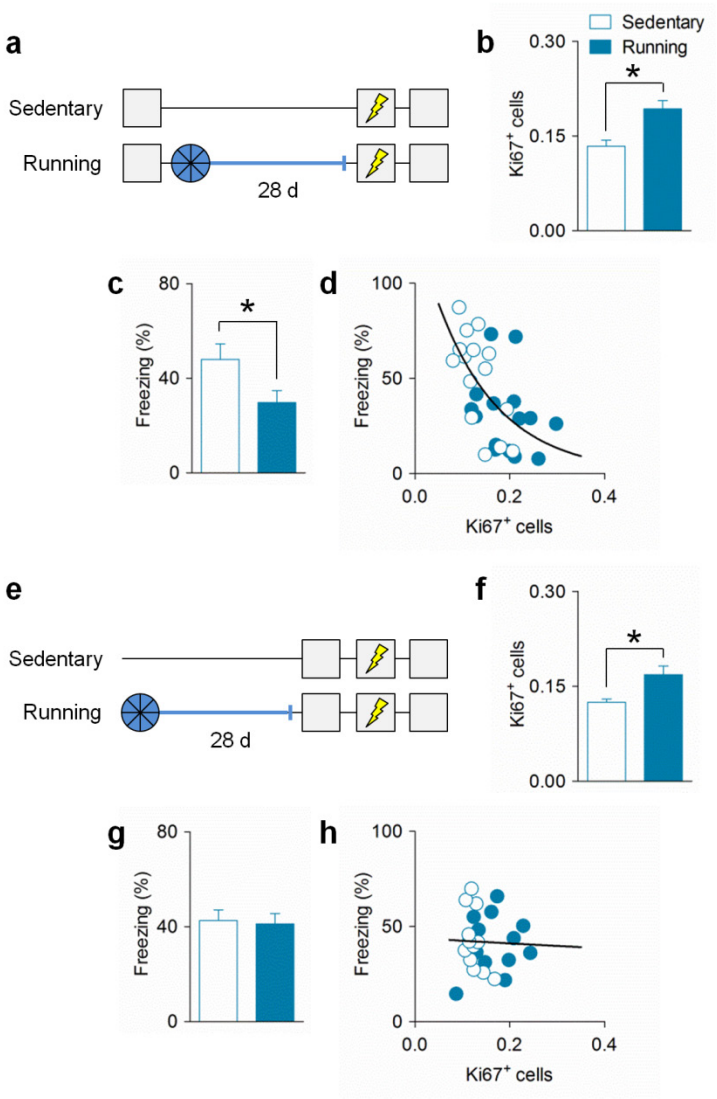

Fig. S13. Post-learning running induces forgetting of a context-only memory in adult (P60) mice. Running after context pre-exposure (**a**) increased the number of proliferating ($Ki67^+$) cells in the DG (**b**; sedentary $n = 15$, running $n = 15$; $t_{28} = 3.62$, $P = 0.001$) and reduced the ability of context pre-exposure to rescue the immediate shock deficit during the test (**c**; sedentary $n = 16$, running $n = 16$; $t_{30} = 2.20$, $P < 0.05$). (**d**) There was an inverse relationship between proliferation ($Ki67^+$ cells) and memory ($r = -0.56$, $P = 0.001$). Running before context pre-exposure (**e**) increased the number of proliferating ($Ki67^+$) cells in the DG (**f**; sedentary $n = 12$, running $n =$

12; $t_{22} = 3.06$, $P < 0.01$), but did not alter the ability of context pre-exposure to rescue the immediate shock deficit during the test (**g**; sedentary $n = 12$, running $n = 12$, $P > 0.05$). (**h**) There was no relationship between proliferation ($Ki67^+$ cells) and memory (freezing score during test) ($r = -0.04$, $P > 0.05$).

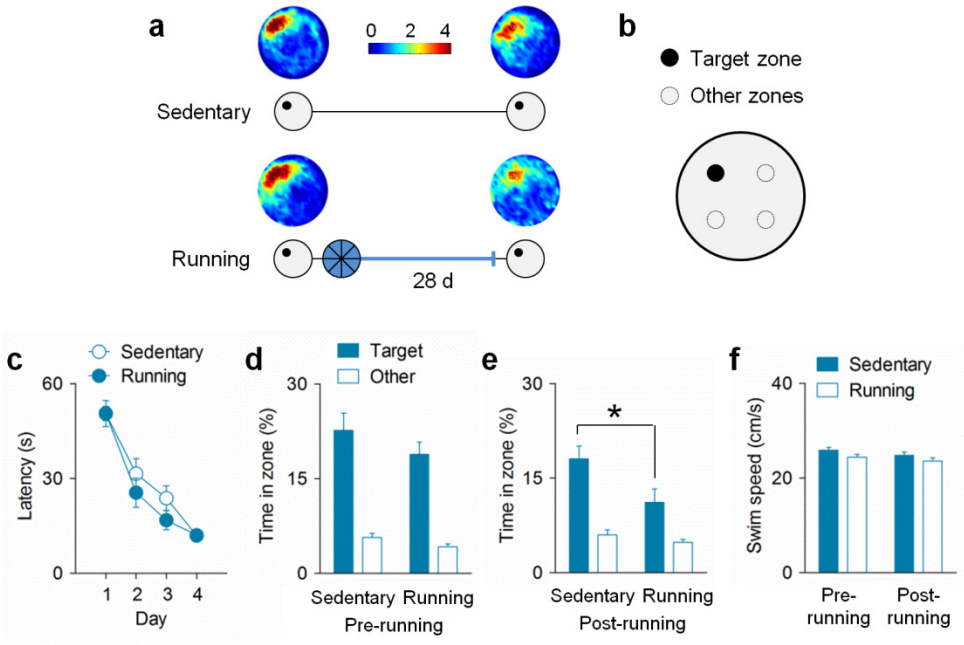

Fig. S14. Post-learning running induces forgetting of a spatial memory. (**a**) Adult (P60) mice were trained to locate a hidden platform in the water maze (density plots show where mice concentrated their search for the platform during probe tests; color legend = average number of visits per mouse per 5 × 5 cm area). (**b**) During probe tests, time spent in a zone (15 cm diameter) that formerly contained the platform (target) was compared with time spent in three other zones. Both groups of mice (**c**) learned to locate the platform during training ($P > 0.05$) and (**d**) exhibited equivalent spatial bias toward the target zone during a pre-running probe test ($P > 0.05$). (**e**) However, mice that ran after water maze training ($n = 16$) showed weaker memory for the platform location during a post-running probe test ($t_{29} = 2.38$, $P < 0.05$) compared with mice that remained sedentary ($n = 15$). (**f**) Sedentary and running mice showed equivalent swim speed during the probe tests ($P > 0.05$).

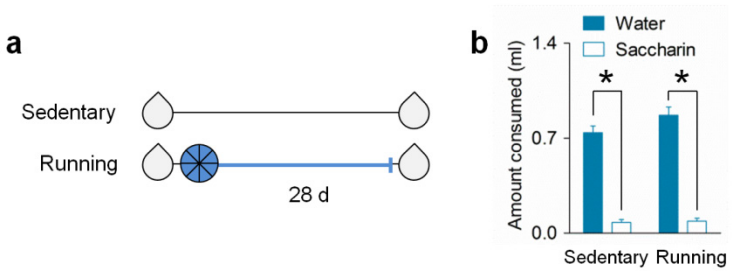

Fig. S15. Running did not lead to forgetting of a non-hippocampal conditioned taste aversion memory. (**a**) Adult (P60) mice were trained to avoid a LiCl-paired saccharin solution, then ran (n = 12) or remained sedentary (n = 12) for 28 days, and then were tested. (**b**) During the test, running and sedentary mice expressed equivalent aversion of the saccharin solution (*fluid* main effect, $F_{1,22} = 309.84$, $P < 0.001$; sedentary, $t_{11} = 13.92$, $P < 0.001$; running, $t_{11} = 11.71$, $P <$ .001).

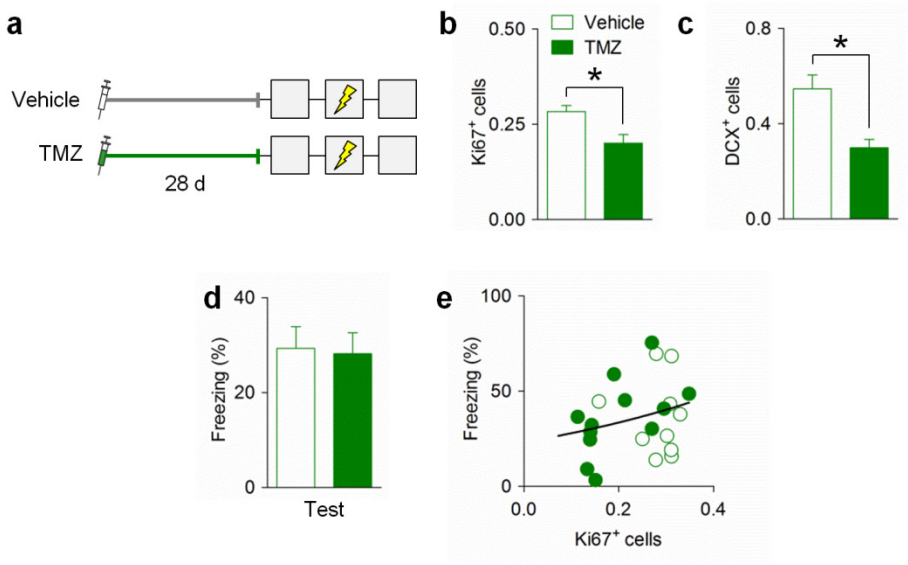

Fig. S16. Disrupting neurogenesis before training did not impact context-only memory in infant (P17) mice. (**a**) Infant mice were treated with vehicle or TMZ before training in the incidental context learning paradigm. TMZ-treated mice had fewer (**b**) proliferating ($Ki67^+$) cells (vehicle n = 10, TMZ n = 12; $t_{20} = 2.92$, $P < 0.01$) and (**c**) immature (DCX^+) neurons (vehicle n = 7, TMZ n = 7; $t_{12} = 3.66$, $P < 0.01$) in the DG compared to vehicle-treated mice. However, infant mice treated with TMZ before training showed no change in freezing during the test (**d**; vehicle n = 22, TMZ n = 22; $P > 0.05$), and there was no relationship between proliferation and freezing (**e**; r = 0.27, $P > 0.05$).

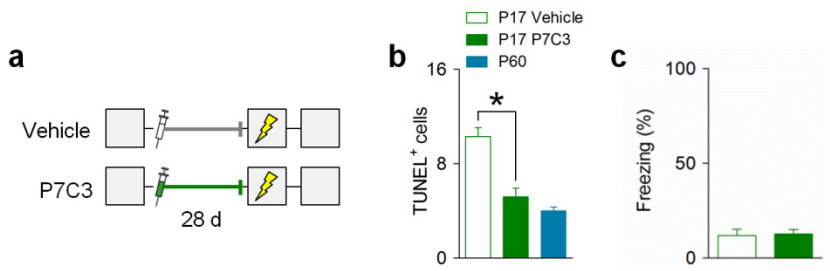

Fig. S17. Reducing cell death in infant mice does not prevent forgetting. (**a**) Infant (P17) mice were pre-exposed to a context and then treated with vehicle (n = 13) or the anti-apoptotic drug P7C3 (n = 13) for 28 days. They were then given immediate shock training and tested 24 hours later. (**b**) P7C3 treatment reduced apoptosis ($TUNEL^+$ cells; vehicle n = 7, P7C3 n = 8; t_{14} = 4.88, $P < .001$) to a level comparable to adults (n = 8) but (**c**) did not alleviate infantile amnesia.

References and Notes

1. W. C. Abraham, A. Robins, Memory retention—the synaptic stability versus plasticity dilemma. *Trends Neurosci.* **28**, 73–78 (2005). Medline doi:10.1016/j.tins.2004.12.003

2. C. Zhao, W. Deng, F. H. Gage, Mechanisms and functional implications of adult neurogenesis. *Cell* **132**, 645–660 (2008). Medline doi:10.1016/j.cell.2008.01.033

3. G. L. Ming, H. Song, Adult neurogenesis in the mammalian central nervous system. *Annu. Rev. Neurosci.* **28**, 223–250 (2005). Medline doi:10.1146/annurev.neuro.28.051804.101459

4. D. A. Laplagne, M. S. Espósito, V. C. Piatti, N. A. Morgenstern, C. Zhao, H. van Praag, F. H. Gage, A. F. Schinder, Functional convergence of neurons generated in the developing and adult hippocampus. *PLOS Biol.* **4**, e409 (2006). Medline doi:10.1371/journal.pbio.0040409

5. N. Toni, D. A. Laplagne, C. Zhao, G. Lombardi, C. E. Ribak, F. H. Gage, A. F. Schinder, Neurons born in the adult dentate gyrus form functional synapses with target cells. *Nat. Neurosci.* **11**, 901–907 (2008). Medline doi:10.1038/nn.2156

6. N. Toni, E. M. Teng, E. A. Bushong, J. B. Aimone, C. Zhao, A. Consiglio, H. van Praag, M. E. Martone, M. H. Ellisman, F. H. Gage, Synapse formation on neurons born in the adult hippocampus. *Nat. Neurosci.* **10**, 727–734 (2007). Medline doi:10.1038/nn1908

7. C. Zhao, E. M. Teng, R. G. Summers Jr., G. L. Ming, F. H. Gage, Distinct morphological stages of dentate granule neuron maturation in the adult mouse hippocampus. *J. Neurosci.* **26**, 3–11 (2006). Medline doi:10.1523/JNEUROSCI.3648-05.2006

8. S. Ge, E. L. Goh, K. A. Sailor, Y. Kitabatake, G. L. Ming, H. Song, GABA regulates synaptic integration of newly generated neurons in the adult brain. *Nature* **439**, 589–593 (2006). Medline doi:10.1038/nature04404

9. Y. Gu, M. Arruda-Carvalho, J. Wang, S. R. Janoschka, S. A. Josselyn, P. W. Frankland, S. Ge, Optical controlling reveals time-dependent roles for adult-born dentate granule cells. *Nat. Neurosci.* **15**, 1700–1706 (2012). Medline doi:10.1038/nn.3260

10. A. Sahay, K. N. Scobie, A. S. Hill, C. M. O'Carroll, M. A. Kheirbek, N. S. Burghardt, A. A. Fenton, A. Dranovsky, R. Hen, Increasing adult hippocampal neurogenesis is sufficient to improve pattern separation. *Nature* **472**, 466–470 (2011). Medline doi:10.1038/nature09817

11. S. S. Stone, C. M. Teixeira, L. M. Devito, K. Zaslavsky, S. A. Josselyn, A. M. Lozano, P. W. Frankland, Stimulation of entorhinal cortex promotes adult neurogenesis and facilitates spatial memory. *J. Neurosci.* **31**, 13469–13484 (2011). Medline doi:10.1523/JNEUROSCI.3100-11.2011

12. P. W. Frankland, S. Köhler, S. A. Josselyn, Hippocampal neurogenesis and forgetting. *Trends Neurosci.* **36**, 497–503 (2013). Medline doi:10.1016/j.tins.2013.05.002

13. M. Yasuda, E. M. Johnson-Venkatesh, H. Zhang, J. M. Parent, M. A. Sutton, H. Umemori, Multiple forms of activity-dependent competition refine hippocampal circuits in vivo. *Neuron* **70**, 1128–1142 (2011). Medline doi:10.1016/j.neuron.2011.04.027

14. K. Deisseroth, S. Singla, H. Toda, M. Monje, T. D. Palmer, R. C. Malenka, Excitation-neurogenesis coupling in adult neural stem/progenitor cells. *Neuron* **42**, 535–552 (2004). Medline doi:10.1016/S0896-6273(04)00266-1

15. L. A. Meltzer, R. Yabaluri, K. Deisseroth, A role for circuit homeostasis in adult neurogenesis. *Trends Neurosci.* **28**, 653–660 (2005). Medline doi:10.1016/j.tins.2005.09.007

16. V. I. Weisz, P. F. Argibay, Neurogenesis interferes with the retrieval of remote memories: Forgetting in neurocomputational terms. *Cognition* **125**, 13–25 (2012). Medline doi:10.1016/j.cognition.2012.07.002

17. H. G. Kuhn, H. Dickinson-Anson, F. H. Gage, Neurogenesis in the dentate gyrus of the adult rat: Age-related decrease of neuronal progenitor proliferation. *J. Neurosci.* **16**, 2027–2033 (1996). Medline

18. T. Seki, Y. Arai, Age-related production of new granule cells in the adult dentate gyrus. *Neuroreport* **6**, 2479–2482 (1995). Medline doi:10.1097/00001756-199512150-00010

19. S. Freud, *Childhood and Concealing Memories*, in *The Basic Writings of Sigmund Freud*, A. A. Brill, Ed. (Norton, New York, 1905), pp. 30–36.

20. B. A. Campbell, in *Comparative Perspectives on the Development of Memory,* R. V. Kail, N. E. Spear, Eds. (Routledge, 1984), pp. 23–35.

21. D. C. Rubin, The distribution of early childhood memories. *Memory* **8**, 265–269 (2000). Medline doi:10.1080/096582100406810

22. B. A. Campbell, N. E. Spear, Ontogeny of memory. *Psychol. Rev.* **79**, 215–236 (1972). Medline doi:10.1037/h0032690

23. L. Acsády, A. Kamondi, A. Sík, T. Freund, G. Buzsáki, GABAergic cells are the major postsynaptic targets of mossy fibers in the rat hippocampus. *J. Neurosci.* **18**, 3386–3403 (1998). Medline

24. J. J. Kim, M. S. Fanselow, Modality-specific retrograde amnesia of fear. *Science* **256**, 675–677 (1992). Medline doi:10.1126/science.1585183

25. K. G. Akers, M. Arruda-Carvalho, S. A. Josselyn, P. W. Frankland, Ontogeny of contextual fear memory formation, specificity, and persistence in mice. *Learn. Mem.* **19**, 598–604 (2012). Medline doi:10.1101/lm.027581.112

26. S. A. Josselyn, P. W. Frankland, Infantile amnesia: A neurogenic hypothesis. *Learn. Mem.* **19**, 423–433 (2012). Medline doi:10.1101/lm.021311.110

27. H. van Praag, G. Kempermann, F. H. Gage, Running increases cell proliferation and neurogenesis in the adult mouse dentate gyrus. *Nat. Neurosci.* **2**, 266–270 (1999). Medline doi:10.1038/6368

28. R. McGonigal, N. Tabatadze, A. Routtenberg, Selective presynaptic terminal remodeling induced by spatial, but not cued, learning: A quantitative confocal study. *Hippocampus* **22**, 1242–1255 (2012). Medline doi:10.1002/hipo.20998

29. H. van Praag, Exercise and the brain: Something to chew on. *Trends Neurosci.* **32**, 283–290 (2009). Medline doi:10.1016/j.tins.2008.12.007

30. Y. Niibori, T. S. Yu, J. R. Epp, K. G. Akers, S. A. Josselyn, P. W. Frankland, Suppression of adult neurogenesis impairs population coding of similar contexts in hippocampal CA3 region. *Nat Commun* **3**, 1253 (2012). Medline doi:10.1038/ncomms2261

31. M. Maekawa, T. Namba, E. Suzuki, S. Yuasa, S. Kohsaka, S. Uchino, NMDA receptor antagonist memantine promotes cell proliferation and production of mature granule neurons in the adult hippocampus. *Neurosci. Res.* **63**, 259–266 (2009). Medline doi:10.1016/j.neures.2008.12.006

32. J. E. Malberg, A. J. Eisch, E. J. Nestler, R. S. Duman, Chronic antidepressant treatment increases neurogenesis in adult rat hippocampus. *J. Neurosci.* **20**, 9104–9110 (2000). Medline

33. N. N. Karpova, A. Pickenhagen, J. Lindholm, E. Tiraboschi, N. Kulesskaya, A. Ágústsdóttir, H. Antila, D. Popova, Y. Akamine, A. Bahi, R. Sullivan, R. Hen, L. J. Drew, E. Castrén, Fear erasure in mice requires synergy between antidepressant drugs and extinction training. *Science* **334**, 1731–1734 (2011). Medline doi:10.1126/science.1214592

34. K. Meletis, V. Wirta, S. M. Hede, M. Nistér, J. Lundeberg, J. Frisén, p53 suppresses the self-renewal of adult neural stem cells. *Development* **133**, 363–369 (2006). Medline doi:10.1242/dev.02208

35. S. A. Josselyn, S. Kida, A. J. Silva, Inducible repression of CREB function disrupts amygdala-dependent memory. *Neurobiol. Learn. Mem.* **82**, 159–163 (2004). Medline doi:10.1016/j.nlm.2004.05.008

36. A. Garthe, J. Behr, G. Kempermann, Adult-generated hippocampal neurons allow the flexible use of spatially precise learning strategies. *PLOS ONE* **4**, e5464 (2009). Medline doi:10.1371/journal.pone.0005464

37. A. Sierra, J. M. Encinas, J. J. Deudero, J. H. Chancey, G. Enikolopov, L. S. Overstreet-Wadiche, S. E. Tsirka, M. Maletic-Savatic, Microglia shape adult hippocampal neurogenesis through apoptosis-coupled phagocytosis. *Cell Stem Cell* **7**, 483–495 (2010). Medline doi:10.1016/j.stem.2010.08.014

38. S. Guidi, E. Ciani, S. Severi, A. Contestabile, R. Bartesaghi, Postnatal neurogenesis in the dentate gyrus of the guinea pig. *Hippocampus* **15**, 285–301 (2005). Medline doi:10.1002/hipo.20050

39. H. Eichenbaum, Hippocampus: Cognitive processes and neural representations that underlie declarative memory. *Neuron* **44**, 109–120 (2004). Medline doi:10.1016/j.neuron.2004.08.028

40. W. Deng, J. B. Aimone, F. H. Gage, New neurons and new memories: How does adult hippocampal neurogenesis affect learning and memory? *Nat. Rev. Neurosci.* **11**, 339–350 (2010). Medline doi:10.1038/nrn2822

41. R. L. Redondo, R. G. Morris, Making memories last: The synaptic tagging and capture hypothesis. *Nat. Rev. Neurosci.* **12**, 17–30 (2011). Medline doi:10.1038/nrn2963

42. X. Liu, S. Ramirez, P. T. Pang, C. B. Puryear, A. Govindarajan, K. Deisseroth, S. Tonegawa, Optogenetic stimulation of a hippocampal engram activates fear memory recall. *Nature* **484**, 381–385 (2012). Medline

43. L. G. Reijmers, B. L. Perkins, N. Matsuo, M. Mayford, Localization of a stable neural correlate of associative memory. *Science* **317**, 1230–1233 (2007). Medline doi:10.1126/science.1143839

44. B. A. Richards, P. W. Frankland, The conjunctive trace. *Hippocampus* **23**, 207–212 (2013). Medline doi:10.1002/hipo.22089

45. J. F. Danker, J. R. Anderson, The ghosts of brain states past: Remembering reactivates the brain regions engaged during encoding. *Psychol. Bull.* **136**, 87–102 (2010). Medline doi:10.1037/a0017937

46. A. Treves, E. T. Rolls, Computational analysis of the role of the hippocampus in memory. *Hippocampus* **4**, 374–391 (1994). Medline doi:10.1002/hipo.450040319

47. B. P. Zambrowicz, A. Imamoto, S. Fiering, L. A. Herzenberg, W. G. Kerr, P. Soriano, Disruption of overlapping transcripts in the ROSA βgeo 26 gene trap strain leads to widespread expression of β-galactosidase in mouse embryos and hematopoietic cells. *Proc. Natl. Acad. Sci. U.S.A.* **94**, 3789–3794 (1997). Medline doi:10.1073/pnas.94.8.3789

48. T. S. Yu, G. Zhang, D. J. Liebl, S. G. Kernie, Traumatic brain injury-induced hippocampal neurogenesis requires activation of early nestin-expressing progenitors. *J. Neurosci.* **28**, 12901–12912 (2008). Medline doi:10.1523/JNEUROSCI.4629-08.2008

49. S. Marino, M. Vooijs, H. van Der Gulden, J. Jonkers, A. Berns, Induction of medulloblastomas in p53-null mutant mice by somatic inactivation of Rb in the external granular layer cells of the cerebellum. *Genes Dev.* **14**, 994–1004 (2000). Medline

50. A. T. Leslie, K. G. Akers, A. D. Krakowski, S. S. Stone, M. Sakaguchi, M. Arruda-Carvalho, P. W. Frankland, Impact of early adverse experience on complexity of adult-generated neurons. *Transl. Psychiatry* **1**, e35 (2011). 10.1038/tp.2011.38 Medline doi:10.1038/tp.2011.38

51. K. Ohira, T. Miyakawa, Chronic treatment with fluoxetine for more than 6 weeks decreases neurogenesis in the subventricular zone of adult mice. *Mol. Brain* **4**, 10 (2011). Medline doi:10.1186/1756-6606-4-10

52. A. A. Pieper, S. Xie, E. Capota, S. J. Estill, J. Zhong, J. M. Long, G. L. Becker, P. Huntington, S. E. Goldman, C. H. Shen, M. Capota, J. K. Britt, T. Kotti, K. Ure, D. J. Brat, N. S. Williams, K. S. MacMillan, J. Naidoo, L. Melito, J. Hsieh, J. De Brabander, J. M. Ready, S. L. McKnight, Discovery of a proneurogenic, neuroprotective chemical. *Cell* **142**, 39–51 (2010). Medline doi:10.1016/j.cell.2010.06.018

53. H. J. G. Gundersen, E. B. V. Jensen, K. Kiêu, Nielsen J, The efficiency of systematic sampling in stereology—reconsidered. *J. Microsc.* **193**, 199–211 (1999). Medline doi:10.1046/j.1365-2818.1999.00457.x

54. G. Kempermann, F. H. Gage, Genetic influence on phenotypic differentiation in adult hippocampal neurogenesis. *Brain Res. Dev. Brain Res.* **134**, 1–12 (2002). Medline doi:10.1016/S0165-3806(01)00224-3

55. A. G. Dayer, A. A. Ford, K. M. Cleaver, M. Yassaee, H. A. Cameron, Short-term and long-term survival of new neurons in the rat dentate gyrus. *J. Comp. Neurol.* **460**, 563–572 (2003). Medline doi:10.1002/cne.10675

56. D. A. Henze, N. N. Urban, G. Barrionuevo, The multifarious hippocampal mossy fiber pathway: A review. *Neuroscience* **98**, 407–427 (2000). Medline doi:10.1016/S0306-4522(00)00146-9

57. D. G. Amaral, J. A. Dent, Development of the mossy fibers of the dentate gyrus: I. A light and electron microscopic study of the mossy fibers and their expansions. *J. Comp. Neurol.* **195**, 51–86 (1981). Medline doi:10.1002/cne.901950106

58. M. Hosseini-Sharifabad, J. R. Nyengaard, Design-based estimation of neuronal number and individual neuronal volume in the rat hippocampus. *J. Neurosci. Methods* **162**, 206–214 (2007). Medline doi:10.1016/j.jneumeth.2007.01.009